Active and Passive Musculature Coupling Strategy to Improve Muscle Strain Prediction

Miguel Corrales, Matheus Correia & Duane Cronin

I. INTRODUCTION

Finite element (FE) Human Body Models (HBMs) can help to assess and analyze the potential for injury risk of vehicle occupants in impact events [1]. Muscle strain has been associated with pain response in the neck under impact loading [2-3]. Current HBM active muscle implementations are generally defined using single 1D uniaxial elements connecting the muscle origin to its insertion [4-5]. In the Global Human Body Model Consortium 50th percentile male v5-1 (M50), the 916 uniaxial elements representing the active muscle were attached to the 3D passive muscle through discrete node sharing. The uniaxial elements approximate the muscle line of action, guided by supporting elements attached to the vertebrae (Fig. 1a). The active musculature and the supporting elements transmit the load to the passive musculature at discrete points leading to uneven passive muscle deformation. In the human body, the active muscle forces are evenly distributed on the passive musculature. In this study, a strategy to improve the distribution of deformation in the 3D passive muscle resulting from coupling with the 1D active muscle was investigated.

II. METHODS

The head-and-neck complex was extracted from the M50 full-body model [1] with active musculature [6] (Fig. 1a). The model included all cervical vertebrae, first thoracic vertebra, intervertebral discs, cervical spine ligaments, 3D passive and 1D active musculature, and a full detailed head.

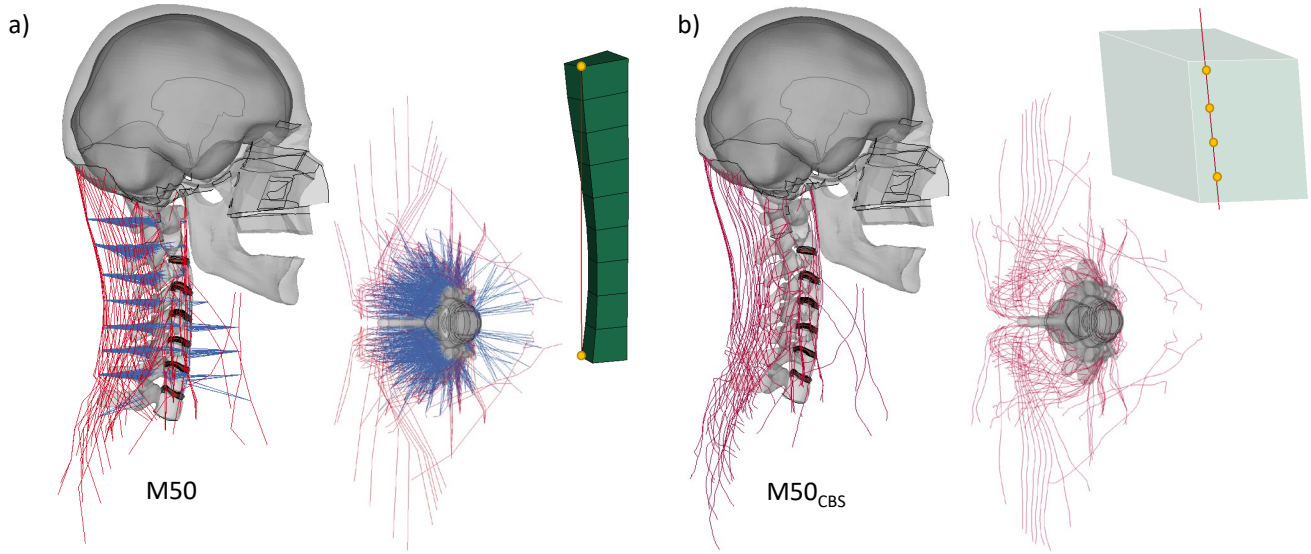

Fig. 1. Sagittal view of the a) M50 and b) $M50_{CBS}$ with bones (grey), active muscle elements (red), and supporting elements (blue); section of the passive musculature of the trapezius (green) demonstrating the passive-active musculature attachment points (yellow) for each implementation.

The supporting elements (Fig. 1a) were removed, then the active muscle mesh was redefined to ensure that the elements passed through the passive musculature with a similar mesh size to the passive muscle elements. The active and passive muscle meshes were attached using a Constrained-Beam-in-Solid (CBS) implementation ($M50_{CBS}$). The CBS method coupled the 1D elements inside the 3D elements through a user-defined number of points (four in this study) along the length of the active muscle elements (Fig. 1b). To modify the active muscle mesh, a custom code was written (Visual Basic for Applications) to generate a set of uniaxial elements that pass through the centre of the passive muscle mesh with a mesh size comparable to the 3D elements. The inputs to the code were a node-set defining the muscle path and the mesh of the corresponding passive muscle mesh. A total of 12,238 uniaxial elements were created to represent the active musculature in the $M50_{CBS}$ compared to 916 in the M50 model.

M. A. Corrales and M. A. Correia are Ph.D. students, and D. S. Cronin (e-mail: duane.cronin@uwaterloo.ca; tel: +1-519-888-4567 x.32682) is a professor, all in the Department of Mechanical and Mechatronics Engineering, University of Waterloo, Canada.

Linear acceleration and rotational displacement boundary conditions from 15 g frontal impact volunteer experiments [5] were applied to the first thoracic vertebrae of the M50 and $M50_{CBS}$ models. The M50 and $M50_{CBS}$ muscle strain (1st principal Green-St. Venant strain) was monitored in the trapezius during the simulations. The distribution and maximum values were compared between the M50 and $M50_{CBS}$ models. In addition, head kinematic responses were compared to the experimental data and to each other.

III. INITIAL FINDINGS

Both the M50 and $M50_{CBS}$ models predicted the maximum strain, measured as the 1st principal Green-St. Venant strain, in the trapezius at 175 ms in the 15 g frontal impact. The 1st principal Green-St. Venant strain predicted by the $M50_{CBS}$ (1.93) was less than two times the strain predicted by the M50 model (5.42) (Fig. 2). The muscle strain of the $M50_{CBS}$ model was found better distributed than that in the M50 model. Importantly, the head kinematic responses of the two models were similar to each other (Fig. 2).

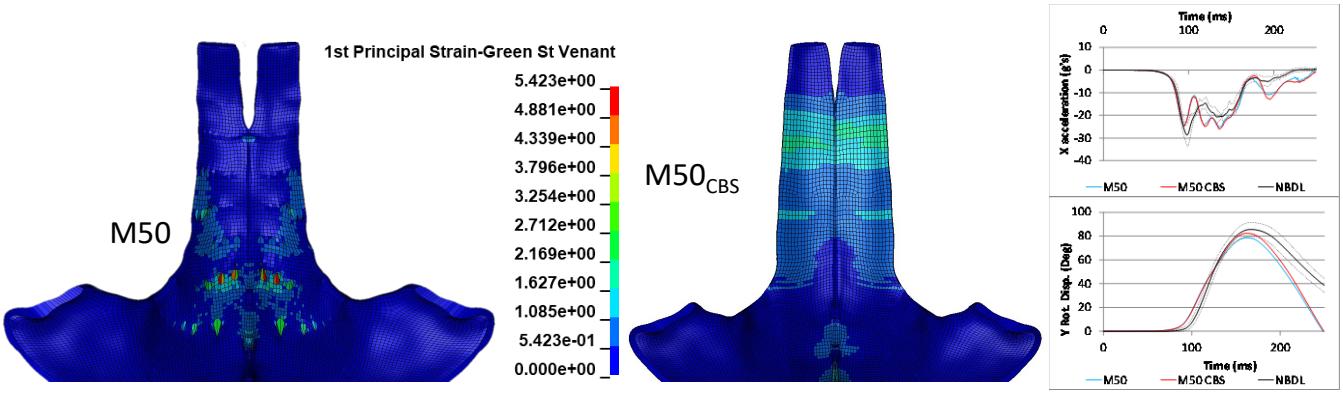

Fig. 2. The M50 and $M50_{CBS}$ trapezius strain at 175 ms and the head kinematic response in a 15 g frontal impact.

IV. DISCUSSION

The CBS implementation improved the distribution of the muscle deformation by continuous coupling of the active and passive elements, rather than discrete connections. The line of action of the 1D active muscles in the $M50_{CBS}$ was maintained using the passive 3D mesh; therefore, the supporting elements were not included in the $M50_{CBS}$ model. In this study, the CBS approach was demonstrated to be equivalent to the supporting elements approach in terms of the head kinematic response. One limitation of the CBS method was the increased number of active elements required (from 916 elements to 12,238 elements). The CBS constraint and increased number of elements in the $M50_{CBS}$, increased the simulation time by almost a factor of 3x; improvement in efficiency by reducing the number of elements and constraints may still be required for general application. The passive muscle strain of the M50 model was being obscured by the effect of the supporting elements and the active muscle attachments at discrete points. The CBS implementation distributed the load of the active musculature uniformly through the passive mesh, while maintaining the head kinematic response, and allowed for assessment of muscle strain in the 3D elements of the $M50_{CBS}$. A link between muscle strain in the model and the potential for injury is included in future work. A more uniform deformation in the muscle of the $M50_{CBS}$ pushes towards soft-tissue-based injury prediction.

V. ACKNOWLEDGEMENTS

The authors gratefully acknowledge the Natural Sciences and Engineering Research Council of Canada, HONDA R&D Americas (HRA-O), General Motors Canada, and the FCA group for the financial support. Thanks to the Global Human Body Models Consortium for use of the HBM and Compute Canada for the computational resources.

VI. REFERENCES

[1] Barker, J., *et al., J Biomech Eng,* 2020.
[2] Brault *et al., Clinical Biomech,* 2000.
[3] Vasavada *et al., Spine,* 2007.
[4] Putra, I, *et al., Ann Biomed Eng,* 2020.
[5] Kato, D, *et al., IRCOBI,* 2016.
[6] Correia, M, *et al., J Biomech,* 2020